Young research workers' prize finalists

A A STUDY OF THE RELATION BETWEEN GAP JUNCTION EXPRESSION, CONDUCTANCE AND CONDUCTION VELOCITY IN INTACT MYOCARDIUM

P. Dhillon[1], A. Shipolini[2], V. Tsang[3], C. Fry[4], N. Peters[1]. [1]*St Mary's Hospital, Imperial College, London, UK;* [2]*The London Chest, Queen Mary and Westfield College, London, UK;* [3]*The Heart Hospital, University College, London, UK;* [4]*University College, London, UK*

Introduction: A conducted myocardial action potential must overcome the tissue intracellular resistivity (R_i) modelled on the gap junction resistivity (R_j) and cytoplasmic resistivity (R_c) in series. Gap junctions are formed from connexin (Cx) proteins of which Cx43 is the major ventricular isoform but both Cx43 and Cx40 are found in atrial tissue. The relation between cardiac gap junction conductance and conduction velocity (CV) in intact tissue remains controversial. Cx gene knockout mice, expressing 50% of wild-type Cx43, have failed to consistently show CV slowing. We tested the hypothesis that a reduction of gap junction conductance (the inverse of Rj) would slow CV in normal myocardium of the guinea-pig. Carbenoxolone, a pharmacological uncoupler, was used as a tool to test this hypothesis. Furthermore we investigated the relation between gap junction expression and conductance in intact human myocardial atrial and ventricular trabeculae.
Methods: *Conduction data.* Action potential and CV in guinea-pig preparations were measured by microelectrode impalement. Carbenoxolone (20 μM) was superfused onto preparations and CV slowing was measured. *Impedance data.* Strips were pulled across a three compartment bath; the middle chamber filled with mineral oil and the outer chambers with oxygenated Tyrode's solution (37C). Alternating current (frequency 20 Hz–300 kHz) was passed along preparations. The longitudinal impedance network analysis provided values for R_i, R_j, and R_c. For guinea-pig experiments some strips were superfused with 20 μM carbenoxolone for 20 minutes prior to impedance analysis. *Connexin quantification.* Measurements were made using standard western blotting techniques.
Results: Gap junction conductance and conduction. Carbenoxolone increased R_i and slowed CV in all chambers (table). Gap junction expression and conductance in human ventricular and atrial myocardium. In the figure (A) shows a negative correlation between Cx43 and Ri and Rj (Pearson r of −0.88 and −0.89 respectively, $p<0.05$ in both cases, n = 7) in the human ventricle. There was no direct relation between the quantity of individual Cx proteins and resistivity (n = 18) in human right atrium. A relative Cx40 expression ratio (Cx40/Cx40+Cx43) was determined for each patient. For individuals with a ratio above 0.75 there was a significant negative linear correlation with R_i/R_j (fig (B)).
Conclusion: In intact normal guinea-pig myocardium, CV is acutely dependent on GJ conductance. In human ventricular specimens the conductance of GJ channels is related in a linear fashion to Cx43 protein expression. In human right atrium a linear negative correlation was seen in individuals expressing a high relative ratio (>75%) of Cx40 in relation to Cx43.

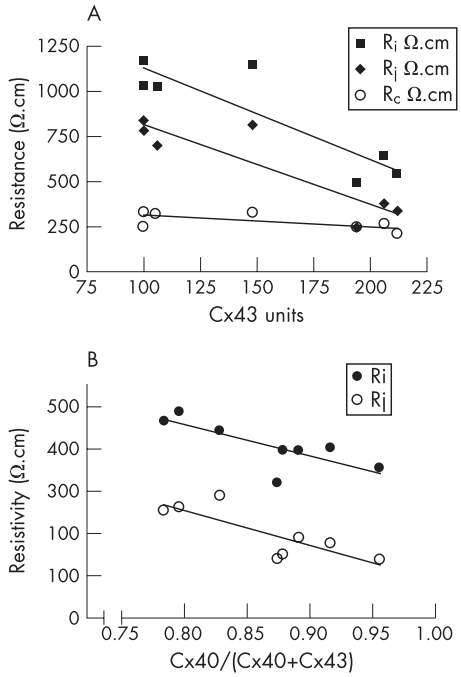

Abstract A.

Abstract A Values (SD) of CVand the intracellular pathway after exposure to carbenoxolone

	LV (n = 6)	LA (n = 6)	RA (n = 6)
CV (cm/s)	59.2 (3.1)* (↓ **17**)	60.1 (6.1)* (↓ **23**)	68.9 (6.7)* (↓ **11**)
R_i (Ω cm)	654 (43)*	331 (22)*	271 (15)*
R_j (Ω cm)	502 (80) * (↑ **28**)	187 (27) * (↑ **27**)	143 (14) * (↑ **21**)
R_c (Ω cm)	152 (41)	144 (18)	127 (16)

Values in parentheses are percentage change from control. Arrows denote an increase or decrease. *$p<0.05$ from control values.

B GENOME-WIDE CELL-SPECIFIC EXPRESSION ANALYSIS IDENTIFIES THE INVOLVEMENT OF THE ADIPOCYTOKINE SIGNALLING PATHWAY IN ATHEROSCLEROTIC PLAQUE RUPTURE

K. Lee[1], T. Polvikoski[2], D. Birchall[2], M. Santibanez-Koref[1], A. Mendelow[2], B. Keavney[1]. [1]*Institute of Human Genetics, University of Newcastle upon Tyne, Newcastle upon Tyne, UK;* [2]*Regional Neurosurgical Centre, Newcastle General Hospital, Newcastle upon Tyne, UK*

Background: The acute events of myocardial infarction and embolic stroke are now understood to be caused by the rupture of the vulnerable atherosclerotic plaque. The molecular mechanisms leading to plaque rupture are still poorly understood. Genome-wide expression studies can analyse many genes simultaneously and may reveal novel molecular pathways of potential pathogenic importance. However due to the heterogeneity in cellular composition between stable and ruptured plaques it is necessary to develop methods of studying the gene expression profiles of specific cell types isolated from the plaques.

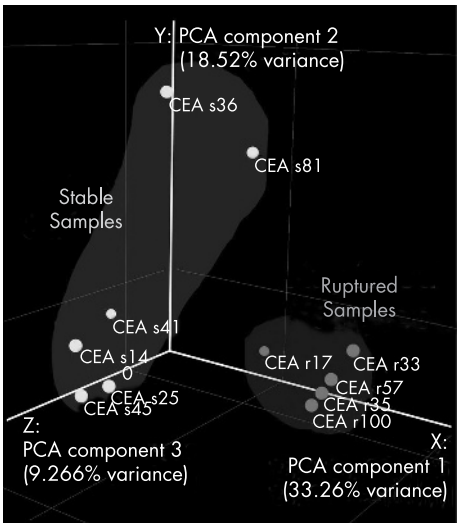

Abstract B Figure 1.

10 most highly expressed genes in ruptured samples

Fold change	Gene symbol
72.06	FABP4
33.58	PABP
25.33	PACAP
24.53	PACAP
11.18	IGO1
10.79	FCGR3A
9.39	IGKLC
9.29	LEP
8.90	HMOX1
8.70	IGKV1D-13

10 most highly expressed genes in stable samples

Fold change	Gene symbol
1/58.8	SFRP4
1/64.5	COL21A1
1/66.7	ITGBL1
1/71.4	COL8A1
1/73.5	ECM2
1/133.2	RGS5
1/143.7	PDGFD
1/153.6	OGN
1/204.5	ASPN
1/229.4	SFRP2

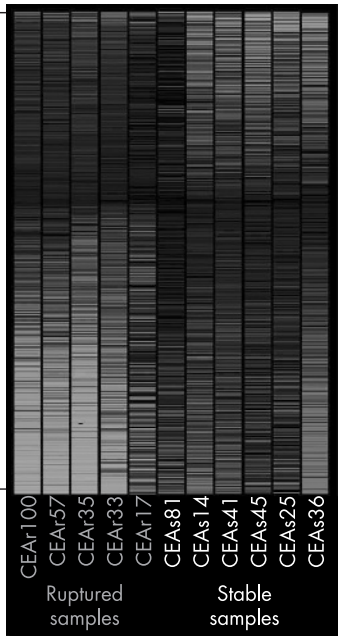

Abstract B Figure 2.

Methods: Snap-frozen human carotid atherosclerotic plaques removed at carotid endarterectomy were designated as stable or ruptured using stringent clinical, radiological and histopathological criteria. Gene expression profiling of macrophages in ruptured and stable plaques was conducted by employing laser micro-dissection to specifically isolate this cell type from the plaques. High quality RNA was used for linear amplification and then hybridised to the genome-wide Affymetrix HG-U133plus2 GeneChip microarray.
Results: Exploratory clustering by principal components analysis showed clear evidence of clustering of the data into two groups; stable and ruptured (fig 1). 889 statistically significant differentially expressed genes were identified and are shown in a heatmap with the 10 most highly expressed genes in the ruptured and stable groups listed (fig 2). Genes involved in lipid processing, signalling, apoptosis, immune response and extracellular matrix interaction were observed to play a role in plaque rupture. Detailed analysis using KEGG pathways identified the adipocytokine signalling pathway to be the most significantly over-represented cell signalling pathway ($p<0.001$), implicating its involvement in plaque rupture for the first time. The adipocytokine leptin was also among the 20 topmost differentially expressed genes. The microarray findings were validated by real-time quantitative PCR with an overall Pearson correlation of $r=0.940$.
Conclusions: Macrophages in stable and unstable atherosclerotic plaques differ not only in number but also in their gene expression profile. This cell-specific genome-wide expression study has identified novel genes and pathways implicated in the contribution of the macrophage to plaque rupture which may be potential biomarkers or therapeutic targets.

C HYPERTROPHIC AND DILATED CARDIOMYOPATHY-CAUSING MUTATIONS OF TROPONIN AND α-TROPOMYOSIN HAVE OPPOSITE EFFECTS ON THIN FILAMENT CALCIUM BINDING

P. Robinson, H. Watkins, C. Redwood. *University of Oxford, Oxford, UK*

Introduction: Inherited hypertrophic (HCM) and dilated (DCM) cardiomyopathy can be caused by mutations in the regulatory proteins of the contractile apparatus. In vitro assays of contractility show that HCM mutations increase the Ca2+ sensitivity of contraction, whereas DCM mutations decrease it. To assess whether these changes are a direct result of altered thin filament Ca2+ affinity, or due to changes in the cooperative interaction of troponin and tropomyosin, we have measured the Ca2+ affinity of the regulatory binding site of cTnC in reconstituted troponin and thin filaments containing either HCM or DCM disease-causing mutations in cTnT, cTnI cTnC and alpha-TM.
Methods: The Ca2+ affinity of the regulatory binding site of cTnC was measured using a fluorescent probe (IAANS) attached to Cys34. Cys34IAANS TnC was incorporated into both troponin complex and reconstituted thin filaments (actin:tropomyosin:troponin at the physiological 7:1:1 ratio). Ca2+ affinities measured using wild type proteins, troponin ($pCa50=6.58$ (0.01)) and thin filaments ($pCa50=6.21$ (0.02)), were in excellent agreement with those reported previously. We have reconstituted Cys34IAANS TnC into either troponin complex or regulated thin filaments with 2 HCM mutations (cTnT Arg92Gln, cTnI Arg145Gly) and 9 DCM mutations (cTnT Arg131Trp, Arg141Trp, Ala172Ser, Arg205Leu, ΔLys210, Asp270Asn; cTnC Gly159Asp; alpha-TM Glu40Lys and Glu54Lys) in order to measure the affect of the mutations on Ca2+ binding.
Results: The Ca2+ affinity of troponin complex was unaffected by the presence of cardiomyopathy-causing mutations with the exception of the cTnI Arg145Gly HCM mutation, which caused an increase in Ca2+ affinity ($\Delta pCa50=+0.31$ (0.05)). When studied in reconstituted thin filaments at physiological 1:1 mutant to wild type protein ratios, all mutations, with the exception of cTnT Asp270Asn, altered Ca2+ binding affinity. This indicates that although cardiomyopathy mutations do not alter cTnC structure, they alter the conformational communication of thin filament regulation and hence affect cooperative Ca2+ binding. HCM mutations increased Ca2+ affinity ($\Delta pCa50=+0.41$ (0.02) to +0.51 (0.01)), while DCM mutations decreased affinity ($\Delta pCa50=-0.54$ (0.04) to -0.12 (0.04)), in a direct correlation with previously reported changes in Ca2+ sensitivity seen with these mutations in in vitro assays of contractility.
Discussion: As TnC is the major Ca2+ buffer in the sarcoplasm it is probable that the increase or decrease in Ca2+ affinity of TnC in thin filaments containing HCM or DCM mutations could directly affect buffering of the Ca2+ transient, with consequences for Ca2+ sensitive remodelling pathways in vivo. The altered Ca2+ signalling may exacerbate the effects of the contractility changes caused by the mutations and contribute to the differing phenotypes.

D DIRECT VASCULAR EFFECTS OF THROMBIN RECEPTOR ACTIVATION IN VIVO IN MAN

I. Gudmundsdottir, C. Ludlam, D. Webb, K. Fox, D. Newby. *University of Edinburgh, Edinburgh, UK*

Introduction: Thrombin is a powerful cardiovascular agonist and a vital link between thrombosis and inflammation. In addition to its role in the coagulation cascade it directly activates platelets, inflammatory cells, endothelium and vascular smooth muscle. Protease activated receptors (PARs) were discovered after an extensive search for a thrombin receptor. In man, PAR-1 appears to be the main human thrombin receptor, whereas PAR-2 is mainly activated by trypsin. PAR-1 antagonists are in clinical development as anti-platelet agents. We here describe for the first time, the direct vascular effects of PAR-1 activation in vivo in man.

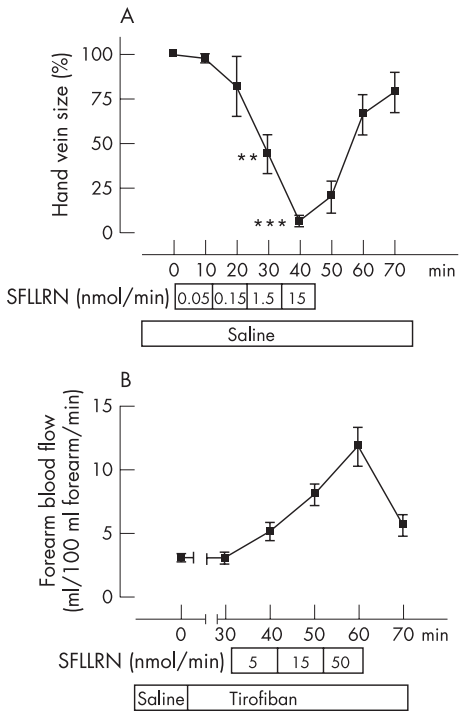

Abstract D Figure 1.

Methods: Dorsal hand vein diameter was measured by the Aellig technique (n = 14) during local intravenous SFLLRN (PAR-1 agonist) and SLIGKV (PAR-2 agonist). SFLLRN was assessed in the presence and absence of norepinephrine and tirofiban, and before and after localised denudation of the venous endothelium (n = 6). Forearm blood flow was measured by venous occlusion plethysmography during intra-arterial SFLLRN, SLIGKV and bradykinin (a control endothelium dependent vasodilator) (n = 16). The mechanism of PAR-1 activation was assessed on 4 visits (n = 8) using a 2×2 factorial design: with and without (a) aspirin (prostacyclin inhibition), or (b) the NO synthase inhibitor L-NMMA co-infused with sodium nitroprusside (the ''NO clamp''). Platelet-monocyte binding and tissue plasminogen activator (tPA), plasminogen activator inhibitor-1 (PAI-1) and von Willebrand factor (vWF) release were measured throughout.

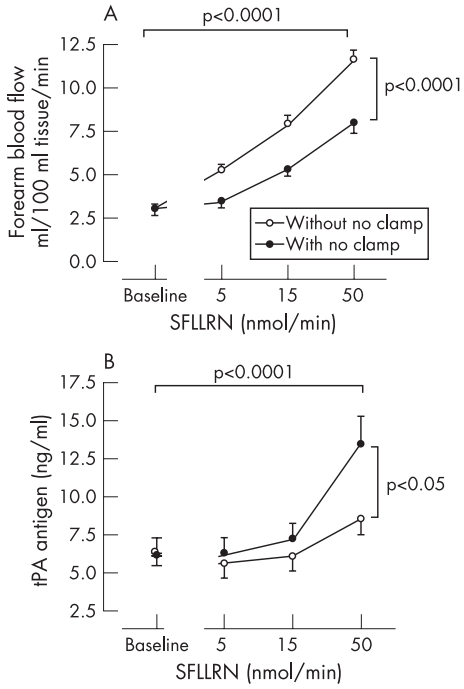

Abstract D Figure 2.

Results: SFLLRN (Fig 1A) and SLIGKV caused venoconstriction and venodilatation respectively ($p<0.001$). SFLLRN induced venoconstriction was unaffected by norepinephrine, tirofiban or endothelial denudation. Arterial SFLLRN increased forearm blood flow (fig 1B, $p<0.001$), platelet-monocyte binding ($p<0.001$), plasma tPA antigen and activity ($p<0.001$), and plasma PAI-1 antigen ($p<0.05$) but not PAI-1 activity or vWF. SLIGKV caused modest arterial dilatation ($p<0.01$) without affecting platelet-monocyte binding or tPA release. SFLLRN induced vasodilatation was reduced by the NO clamp (fig 2A) but not affected by prostacyclin inhibition. SFLLRN induced platelet-monocyte binding was unaffected by NO clamp, aspirin, or tirofiban. Inhibition of NO synthesis, but not prostacyclin, augmented PAR-1 induced tPA release (fig 2B).

Conclusions: PAR-1 activation in vivo in man causes arterial dilatation, venoconstriction, platelet activation and tPA release that is mediated through diverse endothelium-dependent and independent pathways. These unique and contrasting effects are of major physiological relevance to the regulation and resolution of intravascular thrombosis. These findings have implications for the development and therapeutic use of PAR-1 antagonists and direct thrombin inhibitors.

E NOVEL OBSERVATION OF REGIONS OF HIGHLY ORGANISED ACTIVATION AND STABLE FREQUENCY DURING CHRONIC ATRIAL FIBRILLATION IN THE HUMAN LEFT ATRIUM: DO THEY REPRESENT FIXED DRIVERS?

J. Jarman, T. Wong, H. Spohr, P. Kojodjojo, J. Davies, O. Segal, D. Francis, D. Davies, V. Markides, N. Peters. *St Mary's Hospital & Imperial College, London, UK*

Introduction: Experimental data in animals and humans have implicated fibrillatory conduction away from localised re-entrant drivers in the mechanism of atrial fibrillation (AF). Non-contact mapping allows us to perform spectral analysis of chronic AF simultaneously throughout the left atrium (LA). We hypothesised that if drivers of AF were present their principle spectral characteristics would be (a) highly organised activation, approximating a sine wave, associated with (b) temporal stability of the dominant frequency (DF), indicating that the frequency of activation remained relatively constant with time.

Methods: In patients undergoing ablation for chronic AF, a non-contact mapping array was deployed in the LA to record AF before ablation. Non-contact electrograms at 256 evenly distributed LA sites were analysed. Far field ventricular components were subtracted using a novel technique and the outputs subjected to fast Fourier transform. The highest power frequency in the 3–15 Hz range was selected as the DF at each site. Five sequential 7-second segments of AF were analysed in each patient. Mean change in DF between successive segments was defined as the DF variability (DFV) at each site. The area under the DF peak and its harmonics divided by the total area under the power frequency spectrum was calculated for each segment and the mean value defined as the organisational index (OI) at that site. OIs were plotted on a 3-dimensional rendition of the LA surface.

Results: Ten patients completed the protocol. Organised areas were defined as sites with OI greater than one standard deviation above the mean. Mean OI for all sites in all patients was 0.41 (0.02) and in organised areas was 0.51 (0.02). Mean DFV was significantly lower in organised areas than for all sites (0.34 (0.04) vs 0.46 (0.04) Hz (mean (SE)); $p<0.001$), indicating greater temporal stability of DF. Mean DF of all segments was also higher in organised areas (6.31 (0.18) vs 6.21 (0.17) Hz; $p<0.01$). Organised areas were most commonly found at the pulmonary vein orifices (12 of 27 sites; 44%).

Implications: Simultaneous spectral mapping throughout the LA during chronic AF led to a unique observation. Consistent with our hypothesis regarding the expected spectral characteristics of localised re-entrant sources driving AF, we observed LA areas in which highly organised activation is associated with significantly greater temporal stability of the DF than in other areas, a finding which would not be expected in a truly chaotic system. If these areas represent drivers of activation, their approximately equal distribution between pulmonary veins and other LA areas is consistent with clinical experience, emphasising the importance of both pulmonary vein isolation as well as additional left atrial substrate modification for effective ablation of chronic AF. Whether these areas could serve as targets to guide left atrial ablation requires evaluation in a prospective clinical trial.

F EVIDENCE FOR MICROVASCULAR DYSFUNCTION IN HYPERTROPHIC CARDIOMYOPATHY: NEW INSIGHTS FROM MULTIPARAMETRIC MRI

S. Petersen[1], M. Jerosch-Herold[2], L. Hudsmith[1], J. Francis[1], J. Selvanayagam[1], S. Neubauer[1], H. Watkins[1]. [1]*John Radcliffe Hospital, Department of Cardiovascular Medicine, University of Oxford, Oxford, UK;* [2]*Advanced Imaging Research Center, Oregon Health & Science University, Portland, OR, USA*

Introduction: Microvascular dysfunction in hypertrophic cardiomyopathy (HCM) may create an ischemic substrate conducive to sudden death, but it remains unknown if extreme hypertrophy is associated with proportionally poorer perfusion reserve. Extreme hypertrophy is an independent risk factor for sudden death in HCM, but the underlying mechanism is unclear. Cardiac MRI of first pass perfusion is an attractive novel methodology to explore the uncertainties regarding myocardial perfusion in HCM. This methodology, validated against microspheres, has superior spatial resolution compared to nuclear imaging methods, allowing quantitative (ml/min/g) assessment of transmural perfusion gradients both at rest and during stress in myocardial segments. Furthermore, these data can be matched not only with myocardial wall thickness but also, for the first time, with the segmental extent of myocardial fibrosis. Comparisons between magnitude of hypertrophy, impairment of perfusion reserve, and extent of fibrosis may offer new insights for future clinical risk stratification in HCM.

Methods and Results: Degree of hypertrophy, myocardial blood flow at rest and during hyperemia (hMBF), and myocardial fibrosis were assessed with MRI in 35 HCM patients (9 male/26 female), and 14 healthy controls (4 male/10 female), aged 18–78 years (mean 42 (SD 14) years) using the AHA LV segment model. Healthy controls and hypertrophic cardiomyopathy patients differed in LV mass index, but not age and gender. Overall, the HCM cohort was considered low risk, according to clinical risk stratification, and was mainly asymptomatic, with 68% in NYHA class I. Resting MBF averaged 0.71 (0.27) ml/min/g in HCM patients, and 0.85 (0.30) ml/min/g in controls. Resting MBF, adjusted for age ($p=0.58$), gender ($p<0.001$) and resting rate pressure product ($p<0.001$), was similar in HCM patients and controls. hMBF was lower in HCM patients (1.84 (0.89) ml/min/g) than in healthy controls (3.42 (1.76) ml/min/g), with a difference of −0.95 (0.30) (SE) ml/min/g; $p<0.001$) after adjusting for multiple variables, including end-diastolic segmental wall thickness ($p<0.001$). In HCM patients, hMBF decreased with increasing end-diastolic wall thickness ($p<0.005$), and preferentially in the subendocardial layer. The frequency of subendocardial hMBF falling below subepicardial hMBF rose with wall thickness ($p=0.045$), as did the incidence of fibrosis ($p<0.001$). The incidence of fibrosis decreased with increasing hMBF ($p<0.01$).

Conclusions: In hypertrophic cardiomyopathy, the coronary vasodilator response is reduced, particularly in the subendocardium, and in proportion to the magnitude of hypertrophy. Microvascular dysfunction and subsequent ischaemia may be an important component of the risk attributable to HCM with substantial hypertrophy.